

Dynamics of Calcium Signal and Leukotriene C₄ Release in Mast Cells Network Induced by Mechanical Stimuli and Modulated by Interstitial Fluid Flow

Wei Yao, Hongwei Yang, Yabei Li and Guanghong Ding*

*Shanghai Key Laboratory of Acupuncture Mechanism and Acupoint Function,
Department of Mechanics and Engineering Science, Fudan University, 220 Handan
Road, Shanghai 200433, China*

Received 30 May 2013; Accepted (in revised version) 14 June 2015

Abstract. Mast cells (MCs) play an important role in the immune system. Through connective tissues, mechanical stimuli activate intracellular calcium signaling pathways, induce a variety of mediators including leukotriene C₄ (LTC₄) release, and affect MCs' microenvironment. This paper focuses on MCs' intracellular calcium dynamics and LTC₄ release responding to mechanical stimuli, explores signaling pathways in MCs and the effect of interstitial fluid flow on the transport of biological messengers and feedback in the MCs network. We use a mathematical model to show that (i) mechanical stimuli including shear stress induced by interstitial fluid flow can activate mechano-sensitive (MS) ion channels on MCs' membrane and allow Ca²⁺ entry, which increases intracellular Ca²⁺ concentration and leads to LTC₄ release; (ii) LTC₄ in the extracellular space (ECS) acts on surface cysteinyl leukotriene receptors (LTC₄R) on adjacent cells, leading to Ca²⁺ influx through Ca²⁺ release-activated Ca²⁺ (CRAC) channels. An elevated intracellular Ca²⁺ concentration further stimulates LTC₄ release and creates a positive feedback in the MCs network. The findings of this study may facilitate our understanding of the mechanotransduction process in MCs induced by mechanical stimuli, contribute to understanding of interstitial flow-related mechanobiology in MCs network, and provide a methodology for quantitatively analyzing physical treatment methods including acupuncture and massage in traditional Chinese medicine (TCM).

AMS subject classifications: 92C10, 92C05, 92C42

Key words: Mast cells, Ca²⁺ signaling, LTC₄ release, interstitial fluid flow, network.

1 Introduction

MCs are an integral component of the mammalian immune system [1], which resident at

*Corresponding author.

Email: weiyao@fudan.edu.cn (W. Yao), 14110290011@fudan.edu.cn (H. W. Yang), 11210290026@fudan.edu.cn (Y. B. Li), m13564899598@163.com (G. H. Ding)

the interface between the body and the external environment (i.e., under the skin and mucosal surfaces), enabling them to respond rapidly to environmental stimuli, and making them "sentinels" of the immune system [2]. Except for the allergic responses to chemical stimuli, they usually respond to mechanical stimuli such as squeeze, friction, massage and acupuncture. These mechanical stimuli not only activate the mechano-sensitive (M-S) ion channels on MCs membrane and induce a cascade of intracellular signaling events, but also affect the microenvironment of MCs and change the interstitial fluid flow [3]. In recent studies it was found that mechanical stimulation at acupoints is associated with MCs' degranulation [4]. Single-channel activity was observed in the excised patch when negative pressure was applied to MCs [5]. Intracellular Ca^{2+} increase and histamine release were found after shear stress is applied on MCs [6]. Even though the mechanism of MCs' activation by mechanical stimuli is unknown, experimental evidences suggest that TRPV (Transient Receptor Potential Cation Channel, Subfamily V) proteins are involved in this process [7]. Western blot analysis revealed there were TRPV proteins expressed on mast cells [8]. Since TRPV proteins are sensory receptors that can regulate cations influx crossing cell membrane, they may convert external mechanical stimuli into changes in second intracellular messenger signals, particularly Ca^{2+} . Local Ca^{2+} entry activates protein kinase C (PKC) and mobilizes calcium from intracellular stores, leads to other mediators' release [9]. These mediators act in several different ways, e.g., histamine can dilate capillary vessels and increase the interstitial fluid flow [3], LTC_4 can activate MCs and produce more LTC_4 [10]. These biochemical processes change MCs' microenvironment and can sustain MCs activation over a period of time.

Mathematical models have been developed for describing biological messengers' propagation in cells network, especially for neural cells [11]. They either assumed passive diffusion through gap juncture between cells or diffusion in extracellular space (EC-S) as the underlying mechanism [12, 13]. But few of them include the effect of convection. Interstitial fluid flow exists in all living tissues. Experiments and simulations have proved there were directional interstitial fluid flow in some loose connective tissues, and acupuncture can accelerate the flow rate [14, 15]. In this paper, we construct a mathematical model for describing intracellular Ca^{2+} propagation and biological messengers (i.e., LTC_4) release in MCs network induced by mechanical stimuli and modulated by interstitial fluid flow. The rest of the paper is organized as follows. In Section 2, we present the MCs network model. In Section 3, we present numerical simulations under a variety of conditions. The effects of the distance between nearby cells, interstitial flow are investigated. Discussion of our results are given in Section 4.

2 Methods

The dynamic process of MCs activation is illustrated in Fig. 1. In the first stage, mechanical stimuli activate MS ion channels on MCs membrane and allow Ca^{2+} entry; local intracellular Ca^{2+} increase activates PKC and increases the sensitivity of secretory granules

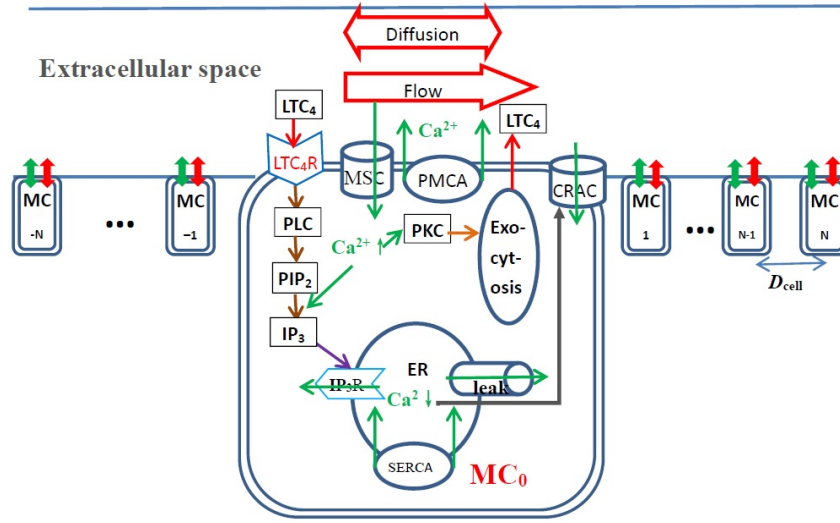


Figure 1: Schematic diagram of the model. MC₀ is the cell activated by mechanical stimuli; the steps leading from MS channel activation to Ca²⁺ release from the calcium store (ER) into the cytosol and LTC₄ release into ECS by exocytosis are described in MC₀. A lane of model MCs (MC₁ means the 1st MC from MC₀ in the flow direction; MC₋₁ means the 1st MC from MC₀ in the contra-flow direction; MC_N means the Nth MC from MC₀ in the flow direction; and MC_{-N} means the Nth MC from MC₀ in the contra-flow direction) are separated by D_{cell} . Each cell exchanges biological messengers through cell membrane with ECS (green arrows represent Ca²⁺, red arrows represent LTC₄). ECS is continuous, diffusion and convection are included.

to Ca²⁺, thus driving exocytosis and LTC₄ release [1]. In the second stage, the released LTC₄ triggers cellular responses through the G-protein linked cysteinyl leukotriene I and II (CysLT₁ and CysLT₂) receptors (LTC₄R) [16]. These receptors bind to phospholipase C (PLC), and PLC catalyzes the hydrolysis of phosphatidylinositol biphosphate (PIP₂) and the release of inositol triphosphate (IP₃) [17]. IP₃ interacts with receptors (IP₃R) on the endoplasmic reticulum (ER), leading to the release of stored Ca²⁺ and the depletion of Ca²⁺ in ER triggers Ca²⁺ entry through Ca²⁺ release-activated Ca²⁺ (CRAC) channels. In the third stage, LTC₄ moves through ECS and activates other MCs.

2.1 Ca²⁺ dynamics

The GHK equation is suitable when there is a large difference in concentrations in the intracellular space (ICS) and ECS compartment, as argued by Koch and Segev [18]. The cross-membrane Ca²⁺ flow is described as

$$I_{Ca,type} = P_{type} \frac{g_{Ca,type} F E_m \left([Ca^{2+}]_i - \exp\left(-\frac{E_m}{\phi}\right) [Ca^{2+}]_e \right)}{\phi \left(1 - \exp\left(-\frac{E_m}{\phi}\right) \right)}, \quad (2.1)$$

where $g_{Ca,type}$ is the permeability of Ca²⁺; F is the Faraday constant; E_m is the membrane potential; $\phi = RT/zF$ is a parameter where R is the universal gas constant, T is

the absolute temperature, z is the valence of ion; $[Ca^{2+}]_i$ and $[Ca^{2+}]_e$ are intracellular and extracellular Ca^{2+} concentration respectively; P_{type} is the proportion of channels in open state: for CRAC channels, $P_{CRAC} = \frac{1}{1+[Ca^{2+}]_{ER}/[Ca^{2+}]_{act1/2}}$ [19], and for MS channels, $P_{MS} = \frac{1}{1+\beta\exp(-\tau)}$ [20]; $[Ca^{2+}]_{ER}$ is the Ca^{2+} concentration in the ER; $[Ca^{2+}]_{act1/2}$ is the concentration for half activation of CRAC channel; β is a measure of the probability that a channel is in the open state in the no-load case; τ is the stimulation intensity. Plasma membrane Ca^{2+} -ATPase (PMCA) extrudes Ca^{2+} to ECS and its flux is given by [21]

$$I_{PMCA} = I_{PMCA,M} \frac{[Ca^{2+}]_i}{K_{PMCA} + [Ca^{2+}]_i}, \quad (2.2)$$

where $I_{PMCA,M}$ is the maximum PMCA flux and K_{PMCA} is the Ca^{2+} concentration for the half activation of PMCA channels. The ER behaves as a Ca^{2+} store and exchanges Ca^{2+} with the cytosol via IP_3 sensitive channels, calcium pumps and leaks. Many models have been developed for these processes, here we follow a model due to Fink et al. [22]. The flux due to IP_3 sensitive channels is

$$J_{IP3} = J_{max} \left(\frac{[IP_3]}{[IP_3] + K_I} \frac{[Ca^{2+}]_i}{[Ca^{2+}]_i + K_{act}} h \right)^3 \left(1 - \frac{[Ca^{2+}]_i}{[Ca^{2+}]_{ER}} \right), \quad (2.3)$$

where J_{max} is the maximum rate, K_I is the dissociation constant for IP_3 binding to IP_3 receptors, K_{act} is the dissociation constant for Ca^{2+} binding to activation sites on IP_3R , h satisfies

$$\frac{dh}{dt} = k_{on} [K_{inh} - ([Ca^{2+}]_i + K_{inh})h], \quad (2.4)$$

where k_{on} is the rate of Ca^{2+} binding to inhibitory sites on IP_3R , and K_{inh} is the corresponding dissociation constant. The SERCA Ca^{2+} pump flux is given by [23]

$$J_{pump} = V_{max} \frac{[Ca^{2+}]_i^2}{[Ca^{2+}]_i^2 + K_p^2}, \quad (2.5)$$

where V_{max} is the maximum pumping rate and K_p is the dissociation constant. The leak flux is given by

$$J_{leak} = P_L \left(1 - \frac{[Ca^{2+}]_i}{[Ca^{2+}]_{ER}} \right), \quad (2.6)$$

where the constant P_L is determined by steady-state flux balance on ER membrane. The cytoplasm Ca^{2+} dynamics is governed by cross-membrane Ca^{2+} flux and Ca^{2+} release from ER

$$\frac{d[Ca^{2+}]_i}{dt} = -\gamma(I_{CRAC} + I_{Ca,MS} + I_{PMCA}) - \gamma \cdot \lambda (J_{IP3} + J_{leak} - J_{pump}), \quad (2.7)$$

where γ is the Ca^{2+} buffering factor [12], λ is the ratio of ER volume to cytoplasm volume. The ER Ca^{2+} dynamics is governed by

$$\frac{d[Ca^{2+}]_{ER}}{dt} = J_{IP3} + J_{leak} - J_{pump}. \quad (2.8)$$

2.2 Secondary messengers' cascade

Agonist-induced activation of the second messengers plays an important role in the mobilization of stored Ca^{2+} inside cells. It starts from the binding of ligands to metabotropic receptors and leads to, via a G-protein cascade, the production of IP_3 and the release of Ca^{2+} from ER [24]. The activated G-protein number $[G]$ is governed by [24]

$$\frac{d[G]}{dt} = k_{aG}(\delta + \rho)([G_T] - [G]) - k_{dG}[G], \quad (2.9)$$

where $[G_T]$ is the total number of G-protein molecules, δ is the ratio of the activities of the unbound and bound receptors[†]. k_{aG} and k_{dG} are the G-protein activation and deactivation rate parameters, respectively. The mediators released from MCs such as LTC_4 , are involved in this process by affecting the fraction of bound receptors, ρ , which is given by $\rho = \frac{[\text{LTC}_4]}{K_R + [\text{LTC}_4]}$, where K_R is the G-protein binding constant. Local Ca^{2+} entry activates PKC [25]

$$\frac{d[\text{PKC}_A]}{dt} = k_{aP}([\text{PKC}_T] - [\text{PKC}_A])[Ca^{2+}]_i - k_{dP}[\text{PKC}_A], \quad (2.10)$$

where $[\text{PKC}_A]$ is the active PKC concentration, $[\text{PKC}_T]$ is the total PKC concentration, k_{aP} and k_{dP} are the PKC activation and deactivation rate parameters, respectively. IP_3 production and degradation is governed by [23]

$$\frac{d[\text{IP}_3]}{dt} = r_h([(\text{PIP}_2)_T] - [\text{IP}_3]) - k_{deg}[\text{IP}_3], \quad (2.11)$$

where $[(\text{PIP}_2)_T]$ is the constant total concentration of PIP_2 , k_{deg} is the IP_3 degradation rate. The production rate r_h depends on activated G-protein and calcium given by $r_h = \alpha[G] \frac{[Ca^{2+}]_i}{K_c + [Ca^{2+}]_i}$ [23], where K_c is the dissociation constant for the Ca^{2+} binding sites on the PLC molecule, α is an effective signal gain parameter, which is determined by solving $\alpha[G] \frac{[Ca^{2+}]_i}{K_c + [Ca^{2+}]_i} ([\text{PIP}_2]_T - [\text{IP}_3]) - k_{deg}[\text{IP}_3] = 0$. Even though the exact mechanism of LTC_4 release from MCs is not known, experimental evidences suggest that local Ca^{2+} entry in MCs activates PKC that triggers the release of LTC_4 into ECS [26]. Shi et al. proposed differential equations describing MC's degranulation based on PKC [25], Bennett et al. established an equation for bio-mediator releasing from astrocytes [12]. In this paper, we combined their methods and assumed LTC_4 released into the extracellular space at a rate

$$V_{\text{LTC}} \xi \max\{[\text{PKC}_A] - [\text{PKC}_A]_{\min}, 0\}, \quad (2.12)$$

[†]This allows for background activity even in the absence of ligand binding, i.e., unbound receptors can activate a small amount of G-protein, therefore the balance value for δ is

$$\delta = \frac{k_{dG}[G]}{k_{aG}([G_T] - [G])} - \rho.$$

where V_{LTC} is LTC_4 production rate. $[PKC_A]_{\min}$ is the threshold concentration, which is necessary to prevent small amounts of $[PKC_A]$ from being amplified and leading to LTC_4 release. ζ is a parameter that accounts for the depletion of LTC_4 inside the cell; it has initial value 1 and decreases according to

$$\frac{\partial \zeta}{\partial t} = -k_{loss} \zeta \frac{\max\{[PKC_A] - [PKC_A]_{\min}, 0\}}{K_{rel} + [PKC_A]},$$

where k_{loss} is the depletion rate parameter, and K_{rel} is the kinetic parameter.

2.3 ECS transport

ECS is considered as a continuum medium, diffusion and convection are both included in describing biological messenger (LTC_4) movement in the MCs network,

$$\frac{\partial [LTC_4]}{\partial t} = D_{LTC} \frac{\partial^2 [LTC_4]}{\partial x^2} - v_{flow} \frac{\partial [LTC_4]}{\partial x} + [LTC_4]_{production}, \quad (2.13)$$

where D_{LTC} is LTC_4 diffusion coefficient, and v_{flow} is the interstitial flow speed. $[LTC_4]_{production}$ is LTC_4 production at location x .

2.4 Parameters and numerical method

Table 1 shows the initial parameter values. Each MC is represented by a ball of diameter $5 \times 10^{-6} \text{m}$ arranged in x direction. The distance between nearby cells $D_{cell} = 3 \times 10^{-5} \text{m}$ for tissues abundant MCs and $D_{cell} = 1.5 \times 10^{-4} \text{m}$ for tissues scarce of MCs. The differential equation (2.13) is solved on a spatial domain $-L < x < L$ where L is chosen to be $3 \times 10^{-3} \text{m}$ in this paper. The equation is first discretized by replacing the partial derivatives in x by difference formulas on equally distributed grid points $-L = x_{-N} < \dots < x_{-2} < x_{-1} < 0 = x_0 < x_1 < x_2 < \dots < x_N = L$ with size δx , the discretization is given by the centered difference formula

$$\begin{aligned} \frac{[LTC_4]_j^{n+1} - [LTC_4]_j^n}{\Delta t} &= \frac{D_{LTC}}{\delta x^2} ([LTC_4]_{j+1}^n - 2[LTC_4]_j^n + [LTC_4]_{j-1}^n) \\ &\quad - \frac{v}{\delta x} ([LTC_4]_{j+1}^n - [LTC_4]_j^n) + [LTC_4]_{production,j}. \end{aligned} \quad (2.14)$$

For $j \geq 0$, $v = v_{flow}$, and for $j < 0$, $v = -v_{flow}$; if there is a MC at location j , $[LTC_4]_{production,j} = V_{LTC} \zeta \max\{[PKC_A]_j^n - [PKC_A]_{\min}, 0\}$, if there is no MC at location j , $[LTC_4]_{production,j} = 0$. This system equation and Eqs. (2.8)-(2.11) are solved using a built-in Matlab solver ode15 with proper initial and boundary conditions. We have carried our simulations by applying mechanical stimuli at $x = 0$.

Table 1: Model parameters and initial resting values.

Parameter	Value	source
g_{CRAC}	$0.3 \Omega^{-1} m^{-2}$	evaluated from [19]
$[Ca]_{act\frac{1}{2}}$	$5 \times 10^{-4} M$	[19]
$g_{Ca,MS}$	$6 \times 10^{-12} Ms^{-1}$	fit for $[Ca^{2+}]_i$ balance
β	99	
$I_{PMCA,M}$	$1.1 \times 10^{-6} M$	fit for [27]
K_{PMCA}	$2.6 \times 10^{-7} M$	fit for [19]
J_{max}	$2.88 \times 10^{-3} M s^{-1}$	[23]
K_I	$3 \times 10^{-8} M$	[23]
k_{on}	$8 \times 10^{-6} M s^{-1}$	[23]
K_{inh}	$10^{-7} M$	[23]
K_{act}	$1.7 \times 10^{-7} M$	[23]
V_{max}	$5.85 \times 10^{-6} M s^{-1}$	[23]
λ	0.08	[28]
K_p	$2.4 \times 10^{-7} M$	[23]
γ	0.0244	[23]
$[G_T]$	1×10^5	[24]
k_{aG}	$0.017 s^{-1}$	[24]
k_{dG}	$0.15 s^{-1}$	[24]
k_{aP}	$0.06 M^{-1}$	[25]
k_{dP}	$0.02 s^{-1}$	[25]
k_{deg}	$1.25 s^{-1}$	[24]
K_c	$4 \times 10^{-7} M$	[24]
V_{LTC}	$0.1 s^{-1}$	fit to experiment [29]
k_{loss}	$30 s^{-1}$	[24]
K_{rel}	$1 \times 10^{-5} M$	[24]
D_{LTC}	$3 \times 10^{-10} m^2 s^{-1}$	[24]
K_{rel}	$1 \times 10^{-5} M$	[24]
v_{flow}	$1 \times 10^{-6} ms^{-1}$	[3]
$[PKC_T]$	$5 \times 10^{-7} M$	[25]
$[(PIP_2)_T]$	$1.66 \times 10^{-7} M$	[24]
$[PKC_A]_{min}$	$1.2 \times 10^{-7} M$	
	Initial values	
$[PKC_A]$	$1 \times 10^{-7} M$	[23]
$[G]$	14	[24]
$[IP_3]$	$10^{-8} M$	[24]
$[Ca^{2+}]_i$	$10^{-7} M$	[25]
$[Ca^{2+}]_e$	$2 \times 10^{-3} M$	[6]
$[Ca^{2+}]_{ER}$	$5 \times 10^{-4} M$	[18]

3 Results

3.1 Single cell response to mechanical stimuli

To validate our model, we first investigate single MC response to mechanical stimuli. Simulation results of Ca^{2+} response to shear stress were plotted in Fig. 2 and were com-

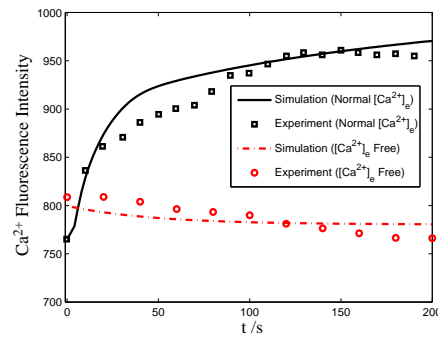


Figure 2: Time-dependent profile of cytosol Ca^{2+} fluorescence intensities in a cell under the stimulation of shear stress. The time 0 represents the beginning of stimulation, open squares represent the experimental data in Hank's buffer ($[\text{Ca}^{2+}]_e = 2 \times 10^{-3} \text{M}$), circles represent the experimental data in the Ca^{2+} -free saline ($[\text{Ca}^{2+}]_e = 0 \text{M}$), solid line represents the simulation results in Hank's buffer and dash line represents the simulation results in the Ca^{2+} -free saline.

pared with experimental data reported in literature [6]. When the cell was stimulated, $[\text{Ca}^{2+}]_i$ gradually increased and was maintained at an elevated level in the presence of extracellular Ca^{2+} ($[\text{Ca}^{2+}]_e = 2 \times 10^{-3} \text{M}$). However, in the absence of extracellular Ca^{2+} ($[\text{Ca}^{2+}]_e = 0 \text{M}$), $[\text{Ca}^{2+}]_i$ didn't increase after the shear stress is applied. These results indicate that the increased $[\text{Ca}^{2+}]_i$ was the Ca^{2+} influx from the ECS through the MS channels.

3.2 MCs network response to mechanical stimuli due to ECS diffusion

We have carried our simulations by applying mechanical stimulate at one MC (MC_0) at $t = 0 \text{s}$. First we considered the case with no interstitial fluid flow ($v_{flow} = 0$ in Eq. (2.13)). Figs. 3-5 show the response (Ca^{2+} & LTC_4 propagation) of MCs network due to ECS diffusion. Cytosol Ca^{2+} responses immediately ($t = 0 \text{s}$) to mechanical stimulate, $[\text{Ca}^{2+}]_i$ increase leads to LTC_4 release and increase in ECS several seconds later ($t = 20 \text{s}$). LTC_4 diffuses in ECS and activates adjacent MCs and spreads. When taking into account not only the diffusion of LTC_4 , but also the synthesis and secretion of LTC_4 from the stimulated cell, there's about 50s latency before the adjacent cells ($30 \times 10^{-6} \text{m}$ or $60 \times 10^{-6} \text{m}$ away) responded. When $v_{flow} = 0$, LTC_4 diffuses equally to downstream (flow direction) and upstream (contra-flow direction), and the Ca^{2+} & LTC_4 waves propagate symmetrically about $x = 0$. Fig. 3 shows the response of MCs network with $D_{cell} = 3 \times 10^{-5} \text{m}$ and a propagation speed of $3.37 \times 10^{-6} \text{ms}^{-1}$, Fig. 4 shows the response of MCs network with $D_{cell} = 6 \times 10^{-5} \text{m}$ and a propagation speed of $2.71 \times 10^{-6} \text{ms}^{-1}$, which is slower than that of $D_{cell} = 3 \times 10^{-5} \text{m}$, Fig. 5 shows the response of MCs network with $D_{cell} = 1.5 \times 10^{-4} \text{m}$ and a the propagation speed of $1.85 \times 10^{-6} \text{ms}^{-1}$, which is even slower. Fig. 6 shows the response of MCs network with $D_{cell} = 3 \times 10^{-4} \text{m}$ and there's no Ca^{2+} & LTC_4 propagation in the network. Figs. 3-5 also show the Ca^{2+} peak in the cellular network decrease with an increased D_{cell} .

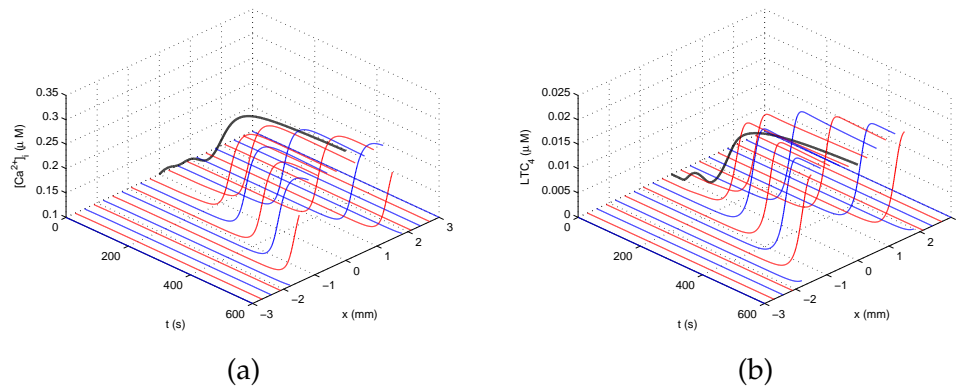


Figure 3: The response of mast cells network of $D_{cell}=3\times 10^{-5}m$ to mechanical stimulate at MC_0 (the mast cell at $x=0$ position) due to diffusion. (a) cytosol Ca^{2+} propagation, (b) extracellular LTC_4 propagation.

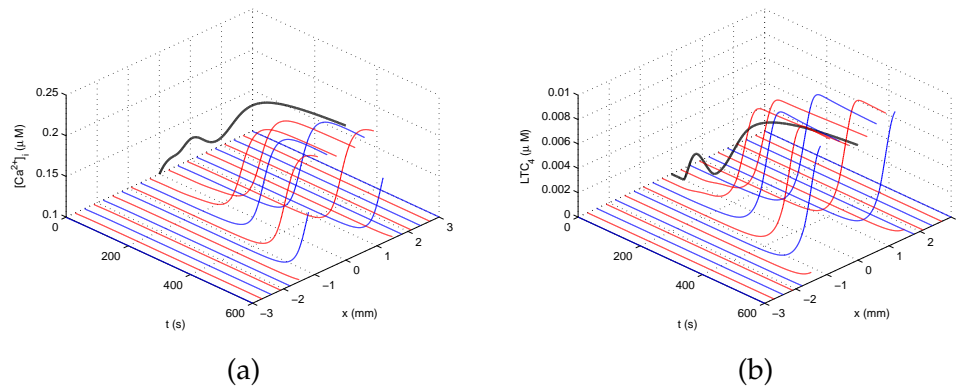


Figure 4: The response of mast cells network of $D_{cell}=6\times 10^{-5}m$ to mechanical stimulate at MC_0 (the mast cell at $x=0$ position) due to diffusion. (a) cytosol Ca^{2+} propagation, (b) extracellular LTC_4 propagation.

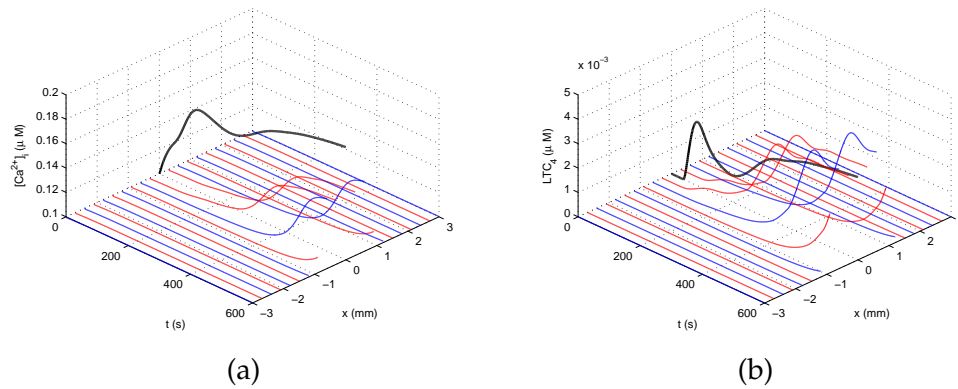


Figure 5: The response of mast cells network of $D_{cell}=1.5\times 10^{-4}m$ to mechanical stimulate at MC_0 (the mast cell at $x=0$ position) due to diffusion. (a) cytosol Ca^{2+} propagation, (b) extracellular LTC_4 propagation.

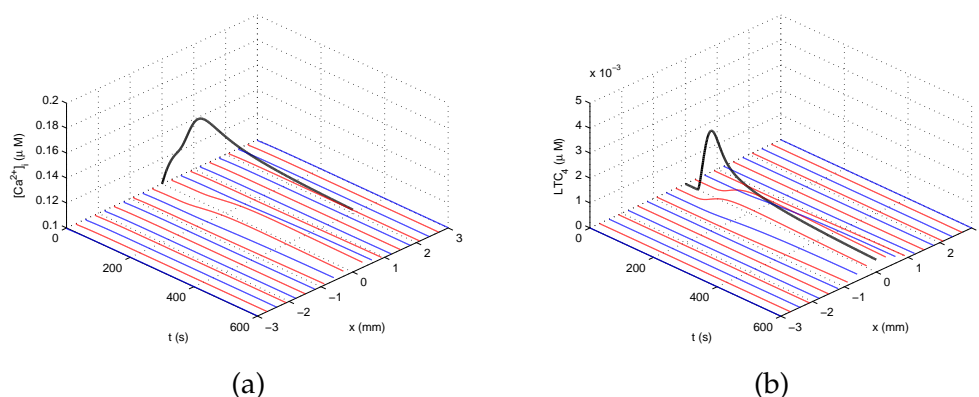


Figure 6: The response of mast cells network of $D_{cell}=3\times 10^{-4}\text{m}$ to mechanical stimulate at MC_0 (the mast cell at $x=0$ position) due to diffusion. (a) cytosol Ca^{2+} propagation, (b) extracellular LTC_4 propagation.

3.3 MCs network response to mechanical stimuli with interstitial flow

We carried the simulations by including both diffusion and convection ($v_{flow} \neq 0$) in ECS. Figs. 7-8 show the response (Ca^{2+} & LTC_4 propagation) of MCs network to mechanical stimuli. The interstitial flow prevented LTC_4 from going upstream ($-x$ direction) and enhanced propagation downstream (x direction). Fig. 7 shows the response for $v_{flow}=1\times 10^{-6}\text{ms}^{-1}$, and the propagation speed in flow direction (downstream) is $4.03\times 10^{-6}\text{ms}^{-1}$, faster than that without flow, while propagation speed in contra-flow direction (upstream) is $2.60\times 10^{-6}\text{ms}^{-1}$, slower than that without flow. Fig. 8 shows the response for $v_{flow}=5\times 10^{-6}\text{ms}^{-1}$, the propagation speed downstream is $6.90\times 10^{-6}\text{ms}^{-1}$, while there was no Ca^{2+} & LTC_4 propagation in the upstream direction. Table 2 compared the propagation speeds and Ca^{2+} peaks under various conditions.

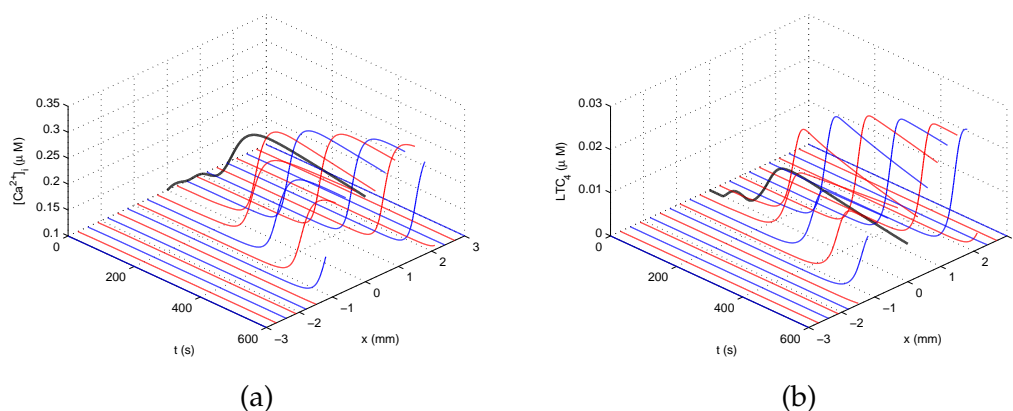


Figure 7: The response of mast cells network of $D_{cell}=3\times 10^{-5}\text{m}$ to mechanical stimulate at MC_0 due to diffusion and convection ($v_{flow}=1\times 10^{-6}\text{ms}^{-1}$). (a) cytosol Ca^{2+} propagation, (b) extracellular biological mediators concentration.

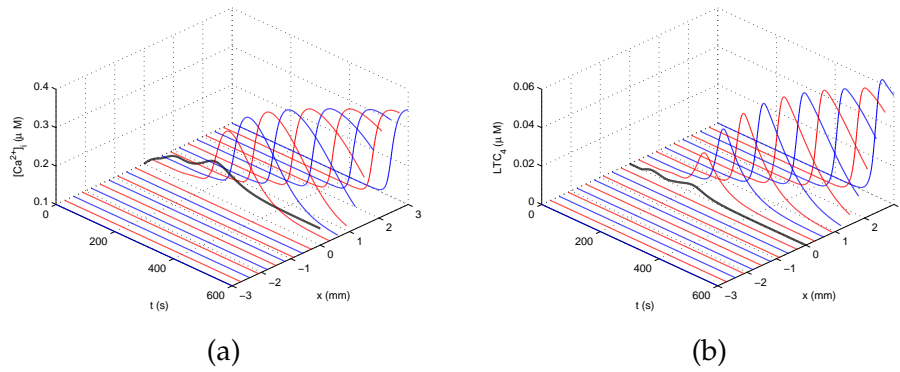


Figure 8: The response of mast cells network of $D_{cell} = 3 \times 10^{-5} \text{m}$ to mechanical stimulate at MC_0 due to diffusion and convection ($v_{flow} = 5 \times 10^{-6} \text{ms}^{-1}$). (a) cytosol Ca^{2+} propagation, (b) extracellular biological mediators concentration.

Table 2: Propagation speeds and Ca^{2+} peaks of waves under different conditions.

types	D_{cell}	Propagation speed	Ca^{2+} peak
Diffusion & $v_{flow} = 0$	$3 \times 10^{-5} \text{m}$	$3.37 \times 10^{-6} \text{ms}^{-1}$	$0.30 \times 10^{-6} \text{M}$
	$6 \times 10^{-5} \text{m}$	$2.71 \times 10^{-6} \text{ms}^{-1}$	$0.24 \times 10^{-6} \text{M}$
	$1.5 \times 10^{-4} \text{m}$	$1.85 \times 10^{-6} \text{ms}^{-1}$	$0.16 \times 10^{-6} \text{M}$
	$3 \times 10^{-4} \text{m}$	No	
Diffusion & $v_{flow} = 1 \times 10^{-6} \text{ms}^{-1}$	$3 \times 10^{-5} \text{m}$	Downstream: $4.03 \times 10^{-6} \text{ms}^{-1}$	$0.32 \times 10^{-6} \text{M}$
		Upstream: $2.60 \times 10^{-6} \text{ms}^{-1}$	$0.24 \times 10^{-6} \text{M}$
Diffusion & $v_{flow} = 5 \times 10^{-6} \text{ms}^{-1}$	$3 \times 10^{-5} \text{m}$	Downstream: $6.90 \times 10^{-6} \text{ms}^{-1}$ Upstream: No	$0.34 \times 10^{-6} \text{M}$

4 Discussion and conclusion

4.1 Mechanical stimuli activate signaling pathway coupling MS channels (TRPV_2) to Ca^{2+} fluxes and biomedical messengers' release in MCs

When shear stress is applied, we have shown with our model that intracellular Ca^{2+} rises and maintains at an elevated level in the presence of extracellular Ca^{2+} , while there is no intracellular Ca^{2+} elevation in the absence of extracellular Ca^{2+} , which is consistent with experiment observations. This results indicate that the increased $[\text{Ca}^{2+}]_i$ was the Ca^{2+} influx from the ECS through the MS channels. Transcripts for a range of TRPVs were detected in MCs [6–8], and we reported the expression of TRPV_2 protein subunits in these cells [7]. We also reported increased membrane currents that could be inhibited by $10 \mu\text{M}$ of ruthenium red (RuR, TRPVs inhibitor) and $20 \mu\text{M}$ SKF96365 (TRPV_2 inhibitor) when negative pressure was applied to MCs (Fig. 9). Influx of extracellular Ca^{2+} through TRPV channels has been demonstrated to be a key step preceding MCs' degranulation [6, 30]. Therefore, we hypothesized that the activation of TRPV_2 to Ca^{2+} fluxes attribute to secondary messengers release induced by mechanical stimuli.

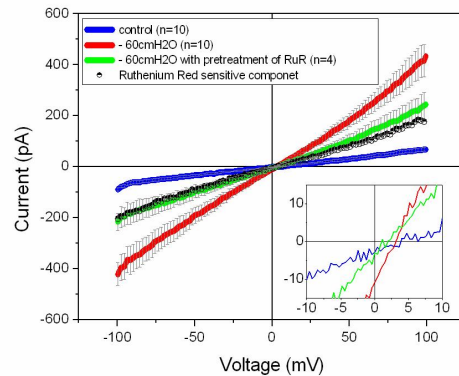


Figure 9: Current-voltage dependence of RuR- sensitive current induced by stretch pressures. Current signals made after activation with/without RuR were compared.

4.2 Biological responses activated by mechanical stimuli can propagate in MCs network due to diffusion and convection in ECS

We have shown with our model that Ca^{2+} & LTC_4 propagation in MCs network ($D_{cell} < 3 \times 10^{-4} \text{m}$) when mechanical stimuli are applied to one MC (Figs. 3-5, Figs. 7-8). It suggests biological signals can propagate in MCs-abundant tissues, i.e., when D_{cell} is small (about $3 \times 10^{-5} \text{m}$). These results may explain the mechanotransduction process in MCs network induced by mechanical stimuli: mechanical stimuli increase $[\text{Ca}^{2+}]_i$ and lead to LTC_4 release; LTC_4 transports (diffuses and flows) in ECS and acts on surface LTC_4R on adjacent cells, leading to Ca^{2+} influx through CRAC channels and increasing $[\text{Ca}^{2+}]_i$, stimulate further LTC_4 production and forms biomedical messengers' signal propagation in the MCs network. When there was no interstitial fluid flow, Ca^{2+} & LTC_4 propagate equally to upstream and downstream, the propagation speeds depended on the value of D_{cell} , and there was no Ca^{2+} & LTC_4 propagation if D_{cell} was too large ($D_{cell} = 3 \times 10^{-4} \text{m}$). Experiment showed a 50 s delay before Ca^{2+} started to rise in the nonpatched mast cells $50-60 \times 10^{-6} \text{m}$ away from the patched (stimulated) mast cell [10]. This is consistent with our simulation results (50s latency before cells $30-60 \times 10^{-6} \text{m}$ away responded). Interstitial fluid flow affects biological signals' propagation. When there was weak interstitial fluid flow ($v_{flow} = 1 \times 10^{-6} \text{ms}^{-1}$), Ca^{2+} & LTC_4 waves propagate faster to downstream (from $3.37 \times 10^{-6} \text{ms}^{-1}$ to $4.03 \times 10^{-6} \text{ms}^{-1}$) and slower to upstream (from $3.37 \times 10^{-6} \text{ms}^{-1}$ to $2.60 \times 10^{-6} \text{ms}^{-1}$). When interstitial fluid flow is significant ($v_{flow} = 5 \times 10^{-6} \text{ms}^{-1}$), there's no Ca^{2+} & LTC_4 propagation in the upstream direction and the propagation speed in the downstream direction increases over 100% ($6.90 \times 10^{-6} \text{ms}^{-1}$).

4.3 MCs network may play a key role in response to mechanical treatment in TCM

Mechanical stimuli have been applied to the body surface for medical treatment, especial-

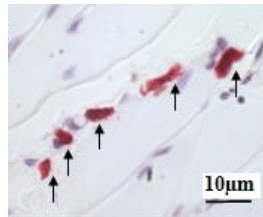


Figure 10: Representative photomicrographs of stained (stained with NR) mast cells (arrows) in specimens at Zusanli (ST36).

ly in TCM. As a basic technique in TCM, acupuncture is a method of applying mechanical stimuli by inserting needles into specific locations (acupoints) where MCs are abundant shown as Fig. 10 [4]. When the needle is twirled, lifted and thrust, the winding of collagen on the acupuncture needle changes the interstitial microenvironment [31, 32]. As we discussed above, mechanical stimuli can activate MCs and lead to the release of biological mediators. These mediators can further activate adjacent cells and induce biomedical messengers' signal propagation in the MCs network. This may explain the acupuncture effect such as "De-qi" (a local sensation of heaviness, numbness, soreness, or paresthesia, which is believed to be an important aspect of treatment), "Xun Jing Gan Chuan" (sensation transport along meridian) and so forth. Moreover, these mediators have a powerful effect in increasing capillary permeability and interstitial flow [3]. On the one hand, an increased flow can induce shear stress on MCs and may activate MCs [6]; On the other hand, the flow can transport biological mediators to downstream locations and activate other MCs along the flow path. Our numerical results showed biomedical messengers' signal propagate equally to both upstream and downstream when there was no flow, while propagate faster to downstream and slower (even none) to upstream when there is a flow. These results can explain the phenomena that sensation propagates in one-direction and can be enhanced by acupuncture.

In this paper, we developed a mathematical model to study Ca^{2+} signaling and LTC_4 release processes, and applied it to investigate the response of MCs network to mechanical stimuli. Extracellular diffusion and convection are both analyzed as underlying mechanisms of biological messenger propagation. This study facilitates our understanding of the mechanotransduction process in MCs induced by mechanical stimuli, contributes to understanding of interstitial flow-related mechanobiology in MCs network and provides a methodology for quantitative analyze mechanical treatments including acupuncture in TCM.

Acknowledgments

This work was supported by National Natural Science Foundation of China (No. 81473750 and No. 11202053), Shanghai Key Laboratory of Acupuncture Mechanis-

m And Acupoint Function (No. 14DZ2260500) and National Basic Research Program of China (No. 2012CB518502).

References

- [1] J. D. CAPITE AND A. B. PAREKH, *CRAC channels and Ca^{2+} signaling in mast cells*, Immunolog. Rev., 231 (2009), pp. 45–58.
- [2] A. WEBER, J. KNOP AND M. MAURER, *Pattern analysis of human cutaneous mast cell populations by total body surface mapping*, British J. Dermatology, 148 (2003), pp. 224–228.
- [3] W. YAO AND G. H. DING, *Interstitial fluid flow: simulation of mechanical environment of cells in the interosseous membrane*, Acta Mech. Sinica, 27 (2011), pp. 602–610.
- [4] D. ZHANG, G. H. DING, X. Y. SHEN, W. YAO, Z. Y. ZHANG, Y. Q. ZHANG, J. LIN AND Q. B. GU, *Role of mast cells in acupuncture effect: a pilot study*, Explore J. Sci. Heal., 4 (2008), pp. 170–177.
- [5] L. N. WANG, G. H. DING, Q. B. GU AND W. SCHWARZ, *Single-channel properties of a stretch-sensitive chloride channel in the human mast cell line HMC-1*, Euro. Biophys. J., 39 (2010), pp. 757–767.
- [6] W. Z. YANG, J. Y. CHEN AND L. W. ZHOU, *Effects of shear stress on intracellular calcium change and histamine release in rat basophilic leukemia (RBL-2H3) cells*, J. Environmental Pathology Oncology, 28 (2009), pp. 223–230.
- [7] D. ZHANG, A. SPIELMANN, G. H. DING AND W. SCHWARZ, *Activation of mast-cell degranulation by different physical stimuli involves activation of the transient-receptor-potential channel TRPV₂*, Physiolog. Res., 61 (2012), pp. 113–124.
- [8] H. TURNER, K. A. DEL CARMEN AND A. STOKES, *Link between TRPV channels and mast cell function*, Handb Exp. Pharmacol., 179 (2007), pp. 457–471.
- [9] H. S. KUEHN AND A. M. GILFILLAN, *G protein-coupled receptors and the modification of Fc_RI-mediated mast cell activation*, Immunology Lett., 113 (2007), pp. 59–69.
- [10] J. L. DICAPITE, A. SHIRLEY, C. NELSON, G. BATES AND A. B. PAREKH, *Intercellular calcium wave propagation involving positive feedback between CRAC channels and cysteinyl leukotrienes*, FASEB J., 23 (2009), pp. 894–905.
- [11] W. YAO, H. HUANG AND R. M. MIURA, *A continuum neuronal model for the instigation and propagation of cortical spreading depression*, Bull. Math. Biol., 73 (2011), pp. 2773–2790.
- [12] M. R. BENNETT, L. FARNELL AND W. G. GIBSON, *A quantitative model of purinergic junctional transmission of calcium waves in astrocyte networks*, Biophys. J., 89 (2005), pp. 2235–2250.
- [13] H. HUANG, R. M. MIURA AND W. YAO, *A simplified neuronal model for the instigation and propagation of cortical spreading depression*, Adv. Appl. Math. Mech., 3 (2011), pp. 759–773.
- [14] H. Y. LI, M. CHEN AND J. F. YANG, *Fluid flow along venous adventitia in rabbits: is it a potential drainage system complementary to vascular circulations?*, Plos. One, 7 (2012), e41395. doi: 10.1371/journal.pone.0041395.
- [15] W. YAO, Y. B. LI AND G. H. DING, *Interstitial fluid flow: the mechanical environment of cells and foundation of meridians*, Evidence-Based Complementary and Alternative Medicine, (2012), Article ID 853516, 9 pages doi:10.1155/2012/853516.
- [16] J. A. BOYCE, *Mast cells and eicosanoid mediators: a system of reciprocal paracrine and autocrine regulation*, Immunol Rev., 217 (2007), pp. 168–185.
- [17] W. YAO, H. X. HUANG AND G. H. DING, *A dynamic model of calcium signaling in mast cells and LTC₄ release induced by mechanical stimuli*, China Sci. Bull., 59 (2013), pp. 956–963.

- [18] C. KOCH AND I. SEGEV, *Methods in Neuronal Modeling: From Ions to Networks*, Cambridge: MIT Press, 1998.
- [19] J. H. SU, F. XU, X. L. LU AND T. J. LU, *Fluid flow induced calcium response in osteoblasts: mathematical modeling*, *J. Biomech.*, 44 (2011), pp. 2040–2046.
- [20] Y. B. YOUMA, J. HANA, N. KIMA, Y. H. ZHANG, E. KIM, H. JOO, H. C. H. LEEM, S. J. KIM, K. A. CHA AND Y. E. EARM, *Role of stretch-activated channels on the stretch-induced changes of rat atrial myocytes*, *Prog. Biophys. Molecular Biology*, 90 (2006), pp. 186–206.
- [21] H. S. SILVA, A. KAPELA AND N. M. TSOUKIAS, *A mathematical model of plasma membrane electro physiology and calcium dynamics in vascularendothelial cells*, *Am. J. PhysiologyCell Physiology*, 293 (2007), pp. 277–293.
- [22] C. F. FINK, B. SLEPCHENKO AND L. M. LOEW, *Determination of time-dependent inositol-1,4,5-trisphosphate concentrations during calcium release in a smooth muscle cell*, *Biophys. J.*, 77 (1999), pp. 617–628.
- [23] M. R. BENNETT, L. FARNELL AND W. G. GIBSON, *A quantitative model of cortical spreading depression due to purinergic and gap-junction transmission in astrocyte networks*, *Biophys. J.*, 95 (2008), pp. 5648–5660.
- [24] G. LEMON, W. G. GIBSON AND M. R. BENNETT, *Metabotropic receptor activation, desensitization and sequestration-I: modelling calcium and inositol 1,4,5-trisphosphate dynamics following receptor activation*, *J. Theor. Biol.*, 223 (2003), pp. 93–111.
- [25] X. M. SHI, Y. F. ZHENG AND Z. R. LIU, *A model of calcium signaling and degranulation dynamics induced by laser irradiation in mast cells*, *China Sci. Bull.*, 53 (2008), pp. 2315–2325.
- [26] W. C. CHANG, C. NELSON AND A. B. PAREKH, *Ca²⁺ influx through CRAC channels activates cytosolic phospholipase A2, leukotriene C4 secretion and expression of c-fos through ERK-dependent and independent pathways in mast cells*, *FASEB J.*, 20 (2006), pp. 2381–2383.
- [27] W. C. CHANG AND A. B. PAREKH, *Close functional coupling between Ca²⁺ release-activated Ca²⁺ channels, arachidonic acid release, and leukotriene C4 secretion*, *J. Biol. Chem.*, 279 (2004), pp. 29994–29999.
- [28] T. MAZEL, R. RAYMOND, M. RAYMOND-STINTZ, S. JETT, B. S. WILSON AND B. BRIDGET, *Stochastic modeling of calcium in 3D geometry*, *Biophys. J.*, 96 (2009), pp. 1691–1706.
- [29] W. C. CHANG, J. D. CAPITE, C. NELSON AND A. B. PAREKH, *All-or-none activation of CRAC channels by agonist elicits graded responses in populations of mast cells*, *J. Immunol.*, 179 (2007), pp. 5255–5263.
- [30] A. J. STOKES, L. M. SHIMODA, M. KOBLAN-HUBERSON, C. N. ADRA AND H. TURNER, *A TRPV₂-PKA signaling module for transduction of physical stimuli in mast cells*, *J. Exp. Med.*, 200 (2004), pp. 137–147.
- [31] H. M. LANGEVIN, D. L. CHURCHILL, J. R. FOX, G. J. BADGER, B. S. GARRA AND M. H. KRAG, *Biomechanical response to acupuncture needling in humans*, *J. Appl. Physiol.*, 91 (2001), pp. 2471–2478.
- [32] X. J. YU, G. H. DING, H. HUANG, J. LIN, W. YAO AND R. ZHAN, *Role of collagen fibers in acupuncture analgesia therapy on rats*, *Connective Tissue Research*, 50 (2009), pp. 110–120.